Colloid Polym Sci (2006) 284: 1387–1393
DOI 10.1007/s00396-006-1507-6

Kabir-ud-Din
Neelam Hazoor Zaidi
Mohd Akram
Zaheer Khan

Mechanism of the oxidation of D-glucose onto colloidal MnO_2 surface in the absence and presence of TX-100 micelles

Received: 8 October 2005
Accepted: 16 March 2006
Published online: 13 June 2006

Kabir-ud-Din (✉) · N. H. Zaidi · M. Akram
Department of Chemistry,
Aligarh Muslim University,
Aligarh 202002, India
e-mail: kabir7@rediffmail.com

Z. Khan
Department of Chemistry,
Jamia Millia Islamia,
Jamia Nagar,
New Delhi 110025, India

Abstract Aqueous colloidal manganese dioxide (MnO_2) was prepared via titration by using potassium permanganate and sodium thiosulphate in aqueous neutral medium. The kinetics of oxidation of D-glucose onto the surface of colloidal MnO_2 have been studied spectrophotometrically. The results show that the rate of initial stage (nonautocatalytic path) increases with increasing the [D-glucose], [H^+], and temperature and also upon addition of nonionic surfactant Triton X-100 (TX-100), which indicates that the surfactant enhances the concentration of D-glucose at the surface of the colloidal MnO_2. Hydrogen bonding interaction seemingly arises between –OH groups of D-glucose and oxygen of the ether linkages of polyoxyethylene chain of TX-100. A possible mechanism of the oxidative degradation of D-glucose is discussed in terms of D-glucose/TX-100 and colloidal MnO_2 interaction.

Keywords Colloidal MnO_2 · Oxidation · D-Glucose · TX-100

Introduction

Carbohydrates are the structural backbone of the DNA, RNA, and nucleic acids and play major role in nutrition. The biochemical importance of the carbohydrates lies in the fact that they form the direct link between the radiant energy emitted by the sun and the demand of living tissues, plant and animal, for supplies of energy required for the purpose of metabolism. They are further important due to their wide occurrence and multihydroxy functionality that allows coordination and chelation to many metal ions. Besides acting simply as effective chelators [1], in many cases, they are also reducing agents [2–5]. Oxidative degradation of sugars by different oxidizing agents has been the subject of numerous investigations [6–13].

Manganese dioxide has been used extensively as an oxidizing agent [14–16] and catalytic agent [17] of both inorganic and organic compounds. Moreover, the transparent solutions of manganese dioxide are also of importance because of their widespread participation as intermediate or reaction products in most permanganate oxidations [18], being actively involved in the mechanism as auto-catalyst in many cases [19]. However, details of the kinetics and mechanism of oxidation of sugars by colloidal manganese dioxide are yet unknown. Therefore, the kinetics and mechanism of the reaction between colloidal MnO_2 and D-glucose both in the aqueous and aqueous-micellar media are reported in this paper.

Experimental

Materials

Triton X-100 (TX-100, 99%, Fluka, Switzerland), potassium permanganate (98.5%, Merck, India), sodium thiosulphate (99%, s.d. fine, India), sulphuric acid (98%, Merck, India) and D-glucose (99%, Merck, India) were used as received. All other salts were of A R grade. Double-distilled and deionized water (specific conductance $1–2\times10^{-6}$ Ω^{-1} cm^{-1}) was used throughout. Standard $KMnO_4$ (5.0×10^{-4} mol dm^{-3}) and sodium thiosulphate (1.87×10^{-4} mol dm^{-3}) were used to prepare the water-soluble colloidal MnO_2 solution [20–22]. The required volume of $KMnO_4$ solution (4.10 cm^3, 9.75×10^{-2} mol dm^{-3}) was added slowly to a standard solution of $Na_2S_2O_3$ (1.38 cm^3, 10.81×10^{-2} mol dm^{-3}) and

the reaction mixture was then diluted by the required volume in 1-dm^3 standard flask. The resulting perfectly transparent dark brown solution was stable for several weeks. The stoichiometric equation is expressed as

$$8MnO^-_4+3S_2O_3^{2-}+2H^+ \rightarrow 8MnO_2+6SO_4^{2-}+H_2O \quad (1)$$

The formation of colloidal MnO_2 was tested by adding a minimum amount of different electrolytes necessary for precipitation of MnO_2.

Kinetic procedure

For each set of kinetic experiments, the requisite volumes of colloidal MnO_2 and H_2SO_4 were taken in a three-necked reaction vessel fitted with a double-surface water condenser to prevent evaporation. A solution of the D-glucose was taken in a separate flask. Both of the solutions were kept thermostated at the experimental temperature (±0.1). The reaction was started by adding a thermally equilibrated requisite volume of D-glucose solution to the reaction mixture. The progress of the reaction was followed by recording the decrease of concentration of colloidal MnO_2 at 390 nm with a B&L Spectronic-20 spectrophotometer up to 80% completion of the reaction. Excess reductant (more than or equal to ten times) was used in all the kinetic runs to maintain pseudo-first-order conditions.

Free radical detection

The presence of free radicals in the reaction mixture was tested by using methylmethacrylate monomer. The addition of the monomer solution (5.0 cm^3) to a reaction mixture containing [MnO_2]=10.0×10^{-3} mol dm^{-3}, [D-glucose]= 10.0×10^{-2} mol dm^{-3}, and [H_2SO_4]=3.72×10^{-4} mol dm^{-3} virtually stopped the reaction, and a white spongy mass appeared. The positive response indicated in situ generation of free radicals in the reaction mixture. Control experiments (with D-glucose or MnO_2 only) did not show any precipitate formation.

Product identification and stoichiometry

Paper chromatography was used for the qualitative identification of the oxidation product of D-glucose [10a, 23]. The D-1,4-gluconolactone was identified as the main product [eluent, *n*-butanol/acetic acid/water (4:1:5)]. The paper chromatograms were visualized by *p*-anisidine reagent [24].

Several reactions mixtures with [MnO_2] < [D-glucose] ([MnO_2]=8.0×10^{-5} mol dm^{-3}; [D-glucose]=2.0×10^{-2} to 12.0×10^{-2} mol dm^{-3}) at fixed [H_2SO_4] (3.0×10^{-4} mol dm^{-3}) were prepared and kept for 2 h at room temperature. The unconsumed MnO_2 was determined spectrophotometrically. The consumption ratio was found to be (MnO_2: D-glucose) 4:1. Due to the autoacceleration nature of the reaction, the exact stoichiometry equation and products formed are difficult to predict (vide-supra).

Results and discussion

Reaction in the absence of TX-100

Preliminary studies

As the plots of log (absorbance) vs time (Fig. 1) deviate from linearity, it is clear that the oxidative degradation kinetics of D-glucose consists of two separate pathways [25, 26]. In the first phase, the reaction follows a nonautocatalytic reaction pathway (oxidation of glucose only). The second phase of the reaction is autocatalytic which may be due to the oxidation of glucose and of its oxidation products. The observed pseudo-first-order rate constants (k_{obs} or k_ψ, s^{-1}) for the initial stages of the reaction were calculated from the slopes of the plots of log (absorbance) vs time. Reproducible results giving good first-order plots (average correlation coefficient, $r \geq 0.998$) were obtained for each kinetic run.

Effect of [H_2SO_4] on the reaction rate

The colloidal MnO_2 solution was found to undergo acid hydrolysis or was unstable in aqueous solution of [H^+] >5.0×10^{-4} mol dm^{-3}. Therefore, the kinetic studies were limited in the [H^+] range of 1.0 to 5.0×10^{-4} mol dm^{-3}. To discover the effect of [H^+] on the pseudo-first-order rate

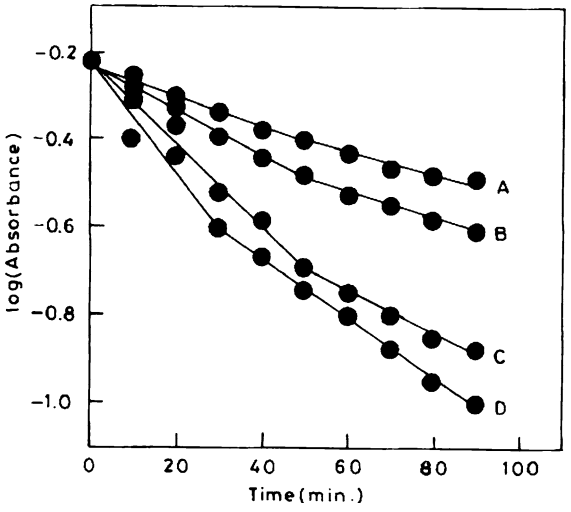

Fig. 1 Plots of log (absorbance) vs time for the oxidation of D-glucose by colloidal MnO_2. Reaction condition [MnO_2]= 8.0×10^{-5} mol dm^{-3}; [D-glucose] 2.0×10^{-2} mol dm^{-3} (**a**), 6.0×10^{-2} mol dm^{-3} (**b**), and 4.0×10^{-2} mol dm^{-3} (**c**, **d**); temperature 30 °C (**a**, **b**), 35 °C (**c**), and 40 °C (**d**)

constant, several kinetic runs were carried out at constant [D-glucose] (4.0×10^{-2} mol dm^{-3}), [MnO_2] (8.0×10^{-5} mol dm^{-3}), and temperature (=30 °C). The reaction was accelerated by an increase in the acidity of the medium (Table 1). k_{obs} vs [H_2SO_4] plot showed a linear relationship with positive intercept on the *Y*-axis (extrapolation until zero concentration of H_2SO_4). It should, however, be zero at [H_2SO_4]=0.0 mol dm^{-3}. Thus, we can conclude that redox reaction has acid-dependent as well as acid-independent paths. It is to be noted that ionic strength of the reaction mixtures could not be maintained constant.

Effect of varying [MnO_2] on the reaction rate

The order with respect to [MnO_2] was determined from the reaction rate obtained at different [MnO_2] and fixed [D-glucose]=4.0×10^{-2} mol dm^{-3} and [H^+]=3.0×10^{-4} mol dm^{-3} at 30 °C (Table 1). The plots of log (absorbance) vs time (Fig. 1) were linear, indicating first-order dependence of the rate on [MnO_2]. This was also confirmed by near-constant values of k_{obs} obtained with varying [MnO_2] (Table 1).

Effect of temperature on the reaction rate

To see the effect of temperature on the reaction rate, a series of kinetic runs was carried out at different temperatures from 25 to 40 °C at fixed [D-glucose] (4.0×10^{-2} mol dm^{-3}), [MnO_2] (8.0×10^{-5} mol dm^{-3}), and [H_2SO_4] (3.0×10^{-4} mol dm^{-3}). The values of k_{obs} were found to fit the Arrhenius equation (Eq. 2) and the plot between log k_{obs} vs 1/ T was linear. The value of activation energy (E_a) was calculated from such plot.

$$\log k_{obs} = \log A - \frac{E_a}{2.303RT} \quad (2)$$

The Eyring equation was used to calculate other activation parameters. The nonlinear least-squares-calculated values of different activation parameters are shown in Table 1. The large negative value of $\Delta S^{\neq}$ shows that the transition state is well structured and highly solvated.

Table 1 Values of pseudo-first-order rate constants (k_{obs}) and activation parameters (E_a, $\Delta H^{\neq}$, and $\Delta S^{\neq}$) for the oxidation of [D-glucose] (4.0×10^{-2} mol dm^{-3}) by colloidal MnO_2 at 30 °C

[MnO_2], 10^5 (mol dm^{-3})	[H_2SO_4], 10^4 (mol dm^{-3})	Temperature (°C)	k_{obs}, 10^4 (s^{-1})
1.6	3.0	30	1.5
3.2			1.5
4.8			1.8
6.4			2.2
8.0			2.5
8.0	1.0	30	1.2
	2.0		1.7
	2.5		2.1
	3.0		2.5
	4.0		2.9
	4.5		3.2
	5.0		3.8
8.0	3.0	25	1.4
		30	2.5
		35	3.6
		40	4.9
Activation parameters			
E_a (kJ mol^{-1})	65		
$\Delta H^{\neq}$ (kJ mol^{-1})	62		
$\Delta S^{\neq}$ (JK^{-1} mol^{-1})	−109		

Table 2 Values of pseudo-first-order rate constants for the oxidation of D-glucose by [MnO_2] (8.0×10^{-5} mol dm^{-3}) in [H_2SO_4] (3.0×10^{-4} mol dm^{-3}) at 30 °C

[D-Glucose], 10^2 (mol dm^{-3})	k_{obs}, 10^4 (s^{-1})	k_{cal}, 10^4 (s^{-1})	$k_{obs}-k_{cal}$/ k_{obs}, 10^4
2.0	1.2	1.2	0.0
4.0	2.5	2.2	+0.12
6.0	2.1	2.8	−0.33
8.0	3.3	3.3	0.0
10.0	3.6	3.7	−0.03
12.0	4.0	4.0	0.0

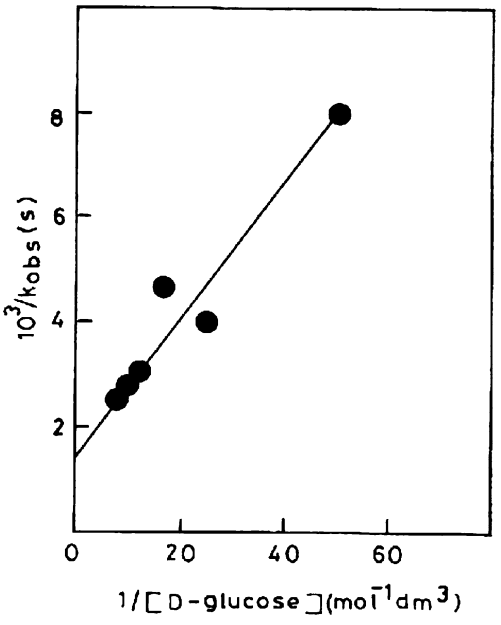

Fig. 2 Plot of $1/k_{obs}$ vs 1/[D-glucose] for the oxidation of D-glucose by colloidal MnO_2. Reaction condition [MnO_2]=8.0×10^{-5} mol dm^{-3}, [H_2SO_4]=3.0×10^{-4} mol dm^{-3}, and temperature=30 °C

Effect of [d-glucose] on the reaction rate

The effect of [D-glucose] was seen under experimental conditions of $[H_2SO_4]=3.0\times10^{-4}$ mol dm^{-3}, $[MnO_2]=8.0\times10^{-5}$ mol dm^{-3}, and temperature=30 °C, which showed rate increase with increase in [D-glucose] (Table 2). The plot of log k_{obs} vs log [D-glucose] was linear with slope=0.70 for the H_2SO_4 concentration used, indicating fractional-order dependence of the rate on [D-glucose]. On the other hand, the plot of k_{obs}^{-1} vs $[\text{D-glucose}]^{-1}$ was also linear at constant $[H^+]$ with a positive intercept and positive slope (Fig. 2). Such a plot is indicative of Michaelis–Menten/Langmuir adsorption isotherm behavior (kinetic proof for complex formation between colloidal MnO_2 and D-glucose).

Scheme 1 $[H^+]$-independent pathway (Eqs. 3, 4, 5, and 6) and $[H^+]$-dependent pathway (Eqs. 7 and 8)

(i) $[H^+]$-independent pathway

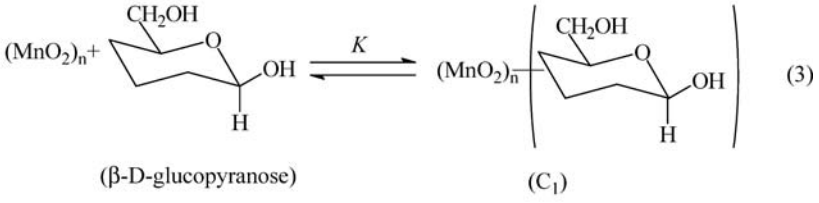

(3)

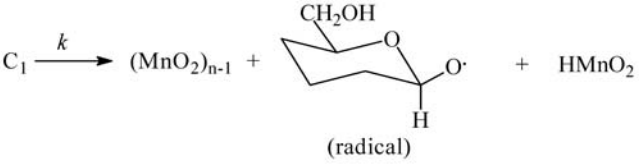

(4)

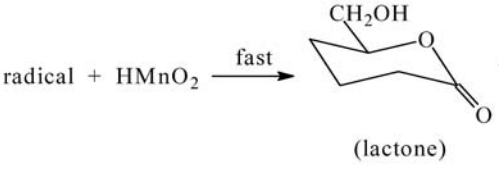

(5)

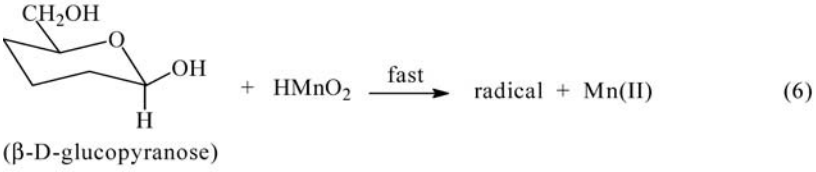

(6)

(ii) $[H^+]$-dependent pathway

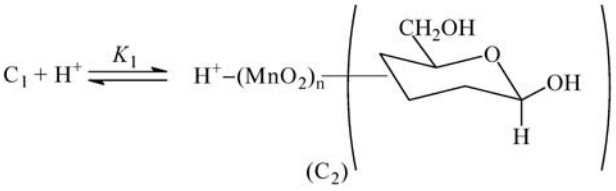

(7)

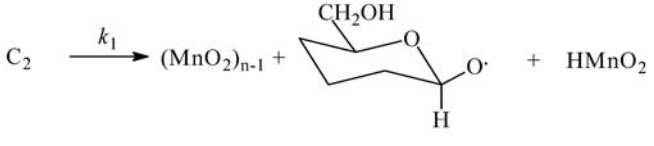

(8)

(reactions (5) and (6) then follow).

Mechanism and rate law

It has been established that, in aqueous solution, D-glucose exists in equilibrium between α- and β-pyranose forms with free aldehyde form as the intermediate [27]. The amount of open-chain form of D-glucose has been estimated from polarographic studies [28] and has been found to be 0.024% at pH 7.0 at 25 °C. On the other hand, the ratio of the α- and β-pyranose forms has been estimated from nuclear magnetic resonance studies [29] at 30 °C to be 36:64.

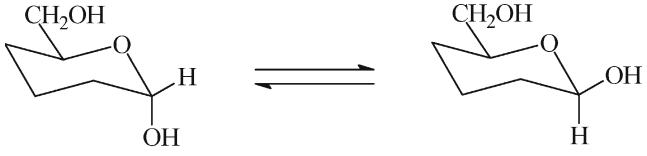

α-D-glucopyranose 36% β-D-glucopyranose 64%

It has also been claimed that the pyranose form is involved in the oxidation reaction. As far as the conformation is concerned, the β-anomer should be more reactive than the α-anomer [30]. Furthermore, the rate of mutarotation is many times greater than the rate of oxidation [27, 31].

On the basis of experimental results, Scheme 1 mechanism has been proposed.

In Scheme 1, Eqs. 3 and 7 represent the adsorption of D-glucose and hydrogen ion on the surface of the colloidal MnO_2 and D-glucose–MnO_2 complex, respectively. Equations 4 and 8 are the respective rate-determining steps. In the light of previous results, we assume that complexes C_1 and C_2 decompose in a one-step, one-electron oxidation–reduction mechanism to manganese(III), radical, and other products. Manganese(III) is a strong oxidant and is unstable with respect to disproportionation. However, we attempted to monitor the formation of manganese(III) at 470 nm but failed to detect any buildup during the course of the reaction.

Scheme 1 mechanism leads to the rate law

$$\upsilon = \frac{-d[\mathrm{MnO_2}]}{d\mathrm{t}} = \frac{\left(kK + k_1K_1K\left[(\mathrm{H^+})_\mathrm{S}\right]\right)\left[(\mathrm{D-glucose})_\mathrm{S}\right][\mathrm{MnO_2}]_\mathrm{T}}{1 + \left(K + K_1K\left[(\mathrm{H^+})_\mathrm{S}\right]\right)\left[(\mathrm{D-glucose})_\mathrm{S}\right]} \tag{9}$$

and

$$k_{obs} = \frac{\left(kK + k_1K_1K\left[(H^+)_S\right]\left[(D-glucose)_S\right]\right.}{1 + \left(K + K_1K\left[(H^+)_S\right]\right)\left[(D-glucose)_S\right]} \tag{10}$$

Under our experimental condition ($[H_2SO_4]=3.0\times10^{-4}$ mol dm^{-3}), the contribution of acid-independent path can be neglected. Thus, Eq. 10 is reduced as Eq. 11.

$$k_{obs} = \frac{k_1K_1K\left[(H^+)_S\right]\left[(D-glucose)_S\right]}{1 + K_1K\left[(H^+)_S\right]\left[(D-glucose)_S\right]} \tag{11}$$

On rearrangement, Eq. 11 can be written as:

$$\frac{1}{k_{obs}} = \frac{1}{k_1K_1K\left[(H^+)_S\right]\left[(D-glucose)_S\right]} + \frac{1}{k_1} \tag{12}$$

A plot of k_{obs}^{-1} vs [D-glucose]$^{-1}$ should accordingly be linear with a positive intercept ($1/k_1$) on the *Y*-axis and a positive slope ($1/k_1K_1K[(H^+)_S]$). This has been found to be so (Fig. 2). Values of k_1 and K_1K were calculated from intercept and slope and found to be 7.14×10^{-4} s^{-1} and 35.91×10^{3} mol^2 dm^{-6}, respectively. On substituting the values of k_1, K_1K, $[H_2SO_4]$, and [(D-glucose)$_S$] in Eq. 11, the calculated values of rate constants (k_{cal}) are obtained for each kinetic run (Table 2). These calculated values of rate constants are in close agreement with the observed pseudo-first-order rate constants (k_{obs}).

Reaction in the presence of TX-100

To see the role of nonionic surfactant, the effect of varying [TX-100] upon the rate of colloidal MnO_2 reduction by D-glucose was studied at constant $[MnO_2]$ (8.0×10^{-5} mol dm^{-3}), [D-glucose] (4.0×10^{-2} mol dm^{-3}), $[H_2SO_4]$ (3.0×10^{-4} mol dm^{-3}), and temperature (30 °C) (Fig. 3). The data so obtained are given in Table 3. The observed effect is catalytic up to a certain [TX-100]; thereafter, an inhibitory effect follows. Tuncay et al. [32] developed a mathematical model for such a catalytic effect. The equation between rate constant (k_ψ) and [TX-100] for the data given in Table 3 for the present reaction is analogously

$$\log k_\psi = 0.2577 \log[TX-100] - 2.9725 (r = 0.988) \tag{13}$$

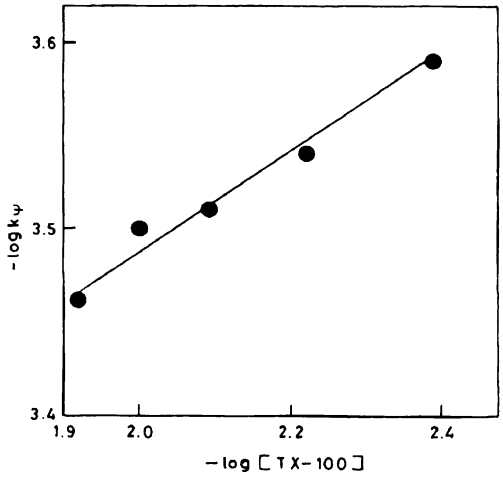

Fig. 3 Plot of log [TX-100] vs log k_{ψ} for the oxidation of D-glucose by colloidal MnO_2. Reaction condition $[MnO_2]=8.0\times10^{-5}$ mol dm^{-3}, [D-glucose]$=4.0\times10^{-2}$ mol dm^{-3}, $[H_2SO_4]=3.0\times10^{-4}$ mol dm^{-3}, and temperature=30 °C

Michaelis–Menten kinetic equation can be used up to catalytic part to explain the observed results. Therefore, the following equation is similar to the Michaelis–Menten type

$$k_{\psi} = k_{obs} + \frac{[TX-100]}{a[TX-100]+b}$$

or

$$k_{\psi} - k_{obs} = \frac{[TX-100]}{a[TX-100]+b} \quad (14)$$

Table 3 Effect of varying the [TX-100] on the k_{ψ} for the oxidation of [D-glucose] (4.0×10^{-2} mol dm^{-3}) by colloidal [MnO_2] (8.0×10^{-5} mol dm^{-3}) in [H_2SO_4] (3.0×10^{-4} mol dm^{-3}) at 30 °C

[TX-100], 10^3 (mol dm^{-3})	$10^4 k_{\psi}$ (s^{-1})
0.0	2.5
4.0	2.6
6.0	2.9
8.0	3.1
10.0	3.2
12.0	3.4
14.0	3.2
16.0	3.1
18.0	2.8

Equation (14) can be rearranged as Lineweaver–Burk form

$$\frac{1}{k_{\psi}-k_{obs}} = a + \frac{b}{[TX-100]} \quad (15)$$

The fulfillment of the above relation can be seen in Fig. 4. The values of a and b were calculated from the slope and intercept of Fig. 4 ($a=1.0\times10^3$ s, $b=133.3$ mol dm^{-3} s) ($r=0.986$).

Probable role of TX-100

It is well known that gum arabic stabilizes colloidal MnO_2 [33], whereas nonionic surfactants enhance the dispersion stability [34]. The catalytic effect of TX-100 indicates that adsorption is not the only factor responsible to explain the effect observed with TX-100 on the oxidation of D-glucose by MnO_2. In addition, the role of other factors, e.g., hydrogen bonding, properties of interfacial water (known to be less polar but more structured than bulk water), differences in stabilization of the initial and transition states by surfactant molecules, reaction rates in the bulk and micellar pseudo-phases, etc., cannot be ruled out completely.

Hydrogen bonding between TX-100 and the reactants may play an important role. D-Glucose possesses no hydrophobic character and has five –OH groups. Hydrogen bonding may occur between the five –OH groups of D-glucose and the ether-oxygen of the polyoxyethylene chains of TX-100. Due to the presence of a number of donor groups in one TX-100 molecule, multiple H-bonding may take place and the number of bound D-glucose molecules increases. In this surfactant, the lengths of the hydrophobic and hydrophilic parts are comparable and have significant amount of water in the

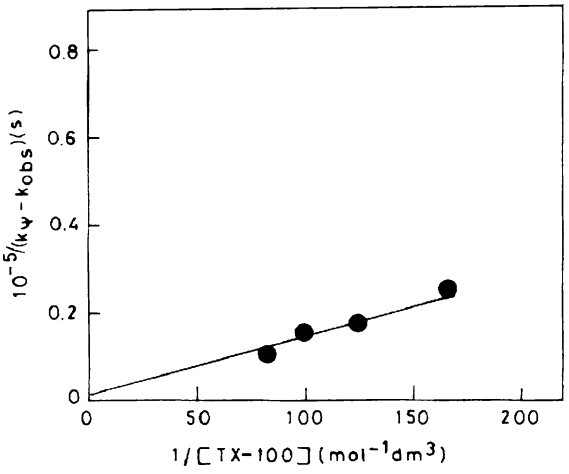

Fig. 4 Plot of $(1/(k_{\psi}-k_{obs}))$ vs 1/[TX-100] for the oxidation of D-glucose by colloidal MnO_2. The reaction condition is the same as in Fig. 3

outer shell. The hydrogen bonding between MnO_2 sols and hydrophilic part (polar ethylene oxide) of the TX-100 cannot be ruled out either (let us call it adsorption). Therefore, the associated MnO_2 and D-glucose with TX-100 (through hydrogen bonding) seems responsible of facilitating the reaction; this might be the role of TX-100 towards the observed catalysis. This surfactant thus helps in bringing the reactants closer, which may orient in a manner suitable for the redox reaction followed by rearrangement of TX-100 molecules. The decrease in rate at higher [TX-100] ($>12.0\times10^{-3}$ mol dm^{-3}) could be due to the 'dilution effect': continuous increase in [TX-100] produces micelles and progressively more and more substrate (D-glucose) gets associated to the micellar phase. This segregation deactivates the substrate as D-glucose in one micelle cannot react with MnO_2 (onto which TX-100 is adsorbed). A point worth noting is that even at [TX-100]= 18.0×10^{-3} mol dm^{-3}, the rate constant is still higher than the values observed in bulk water (Table 3); this proves beyond doubt that TX-100 is still playing its role in catalyzing the reaction.

Conclusion

The catalytic role of nonionic surfactant TX-100 for the oxidation of D-glucose by colloidal MnO_2 has been reported for the first time. The reaction proceeds through the adsorption of D-glucose on the surface of the colloidal particles. The catalytic effect of TX-100 may be due to multiple H-bonding between the surfactant and the reactants (MnO_2 and D-glucose).

References

1. Angyal S (1989) Adv Carbohydr Chem Biochem 47:1–43
2. Sala LF, Cirelli A, Lederkremer R (1977) J Chem Soc Perkin Trans 2:685–688
3. Sala LF, Cirelli A, Lederkremer R (1978) Anal Asoc Quim Arg 66:57–63
4. Gupta M, Saha S, Banerjee PJ (1988) J Chem Soc Perkin Trans 2:1781–1785
5. Barek J, Berka A, Pokorna-Hladikova (1982) Collect Czech Chem Comm 47:2446–2477
6. Singh SV, Saxena OC, Singh MP (1970) J Am Chem Soc 92:537–541
7. Isbell HS, Frush HL (1973) Carbohydr Res 28:295–301
8. Mehrotra RN, Amis ES (1974) J Org Chem 39:1788–1791
9. Kumar A, Mehrotra RN (1975) J Org Chem 40:1248–1252
10. (a) Sen Gupta KK, Sen Gupta S, Basu SN (1979) Carbohydr Res 71:75–84, (b) Sen Gupta KK, Basu SN (1980) Carbohydr Res 80:223–232, (c) Sen Gupta KK, Basu SN (1980) Carbohydr Res 86:7–16
11. (a) Sala LF, Signorella SR, Rizzotto M, Frascaroli MI, Gandolfo F (1992) Can J Chem 70:2046–2052, (b) Signorella SR, Rizzotto M, Daier V, Frascaroli MI, Palopoli C, Martino D, Bousseksou A, Sala LF (1996) J Chem Soc Dalton Trans, pp 1607–1611
12. Virtanen POI, Kurkisuo S (1985) Carbohydr Res 138:215–223
13. Kistayya T, Reddy MS, Kandlikar S (1986) Indian J Chem 25A:905–907
14. Sharma TC, Lal A, Saksena V (1976) Bull Chem Soc Jpn 49:289–291
15. Basak B, Malati MA (1977) J Inorg Nucl Chem 39:1081–1084
16. Taniguchi S (1984) Bull Chem Soc Jpn 57:2683–2684
17. Abd El-Salaam KM (1975) Z Phys Chem 95:139–146
18. Freeman F, Kappos JC (1985) J Am Chem Soc 107:6628–6633
19. Perez-Benito JF, Lee DG (1985) Can J Chem 63:1275–1279
20. Perez-Benito JF, Brillas E, Pouplana R (1989) Inorg Chem 28:390–392
21. Perez-Benito JF, Arias C (1992) J Colloid Interface Sci 149:92–97
22. Perez-Benito JF, Arias C, Amat E (1996) J Colloid Interface Sci 177: 288–297
23. Sala LF, Signorella SR, Rizzotto M, Frascaroli MI (1992) Can J Chem 70:2046–2052
24. Sala LF, Palopoli C, Signorella S (1995) Polyhedron 14:1725–1730
25. Pare B, Pipada M, Choube A, Bhagwat VW (2003) Oxid Commun 26:95–104
26. Khan Z, Raju, Akram M, Kabir-ud-Din (2004) Int J Chem Kinet 36:359–366
27. Virtanen POI, Kurkisuo S, Nevala H, Pohjola S (1986) Acta Chem Scand A Phys Inorg Chem 40:200–206
28. Cantor SM, Peniston QP (1940) J Am Chem Soc 62:2113–2121
29. Rudrum M, Shaw DF (1965) J Chem Soc, pp 52–57
30. Perlin AS (1964) Can J Chem 42:2365–2374
31. Mehrotra R, Kumar A (1976) J Org Chem 40:1248–1252
32. Tuncay M, Yuce N, Arlkan B, Gokturk S (1999) Colloids Surf A Physicochem Eng Asp 149:279–284
33. Tompkins FC (1942) Trans Faraday Soc 38:131–139
34. Cummins PG, Staples E, Penfold J (1990s) J Phys Chem 94:3740–3745